

Summary and Outlook of “How Low Can CT Dose Go”?

Marc Kachelrieß

German Cancer Research Center (DKFZ)

Heidelberg, Germany

www.dkfz.de/ct



DEUTSCHES
KREBSFORSCHUNGSZENTRUM
IN DER HELMHOLTZ-GEMEINSCHAFT



Total Dose Reduction

Additionally Possible Compared to Today's CTs

- Risk-specific AEC (Joscha Maier)
 - about 10%, depending on the tube voltage
- Optimized spectra (Michael McNitt-Gray)
 - 20% to 50% with Sn prefilters for unenhanced depending on object size
 - ??? for enhanced scans
- Dynamic bowtie (Grace Gang)
 - 27% to 50%
- Photon counting:
 - ???
- Deep learning instead of iterative recon
 - ???

Dose Reduction by Patient-Specific Tin or Copper Prefilters^{1,2}



	Child (15 cm × 10 cm)	Adult (30 cm × 20 cm)	Obese (50 cm × 40 cm)
Basis (no filter)	30 mAs	100 mAs	600 mAs
Soft tissue, Sn	0.8 mm / 5000 mAs / 15% → 17%	1.6 mm / 5000 mAs / 33% → 34%	1.5 mm / 5000 mAs / 48% → 57%
Soft tissue, Cu	1.7 mm / 5000 mAs / 16% → 17%	4.5 mm / 5000 mAs / 33% → 34%	4.5 mm / 5000 mAs / 47% → 57%
Iodine, Sn	0 / 30 mAs / 0%	0.2 mm / 1300 mAs / 14%	0.3 mm / 5000 mAs / 29% → 33%
Iodine, Cu	0.6 mm / 5000 mAs / 39% → 42%	1.2 mm / 5000 mAs / 37% → 42%	0.5 mm / 5000 mAs / 30% → 52%

- **Soft tissue CNRD in single energy CT:**

- Can be maximized by choosing the Sn or Cu prefilter as thick as the tube power allows to.

- **Iodine CNRD in single energy CT:**

- Cu prefilter thickness should be adapted to the patient size (zero for children, small for adults, as thick as tube power allows for obese).
- Sn prefilter thickness should be adapted to the patient size (zero for children, small for adults, as thick as tube power allows for obese).

This confirms the dose reduction values reported by Michael McNitt-Gray for unenhanced scans also for enhanced scans (but with Cu instead of Sn)

- **Deviating from the optimal Sn filter thickness by 0.1 mm results in a dose increase of up to 4%.**

¹Steidel, Maier, Sawall, Kachelrieß. Tin or Copper Prefilters for Dose Reduction in Diagnostic Single Energy CT? RSNA 2020.

²Steidel, Maier, Sawall, Kachelrieß. Dose Reduction through Patient-Specific Prefilters in Diagnostic Single Energy CT. RSNA 2020.

Dose Reduction by Photon Counting

- Numerous publications (next slides)

Willemink et al. (Review Paper)

This copy is for personal use only.
To order printed copies, contact reprints@rsna.org

REVIEWS AND COMMENTARY • REVIEW

Photon-counting CT: Technical Principles and Clinical Prospects

Martin J. Willemink, MD, PhD • Mats Persson, PhD • Amir Pourmorteza, PhD • Norbert J. Pelc, ScD • Dominik Fleischmann, MD

From the Department of Radiology (M.J.W., M.P., N.J.P., D.F.) and Stanford Cardiovascular Institute (D.F.), Stanford University School of Medicine, 300 Pasteur Dr, S-072, Stanford, CA 94305-5105; Department of Radiology, University Medical Center Utrecht, Utrecht, the Netherlands (M.J.W.); Departments of Bioengineering (M.P., N.J.P.) and Electrical Engineering (N.J.P.), Stanford University, Stanford, Calif; Department of Radiology and Department of Imaging Sciences and Biomedical Informatics, Emory University School of Medicine, Atlanta, Ga (A.P.). Received November 15, 2017; revision requested January 2, 2018; final revision received January 23; accepted February 5. Address correspondence to M.J.W. (e-mail: m.j.willemink@stanford.edu).

Conflicts of interest are listed at the end of this article.

Radiology 2018; 289:293–312 • <https://doi.org/10.1148/radiol.2018172656> • Content code: CT

Photon-counting CT is an emerging technology with the potential to dramatically change clinical CT. Photon-counting CT uses new energy-resolving x-ray detectors, with mechanisms that differ substantially from those of conventional energy-integrating detectors. Photon-counting CT detectors count the number of incoming photons and measure photon energy. This technique results in higher contrast-to-noise ratio, improved spatial resolution, and optimized spectral imaging. Photon-counting CT can reduce radiation exposure, reconstruct images at a higher resolution, correct beam-hardening artifacts, optimize the use of contrast agents, and create opportunities for quantitative imaging relative to current CT technology. In this review, the authors will explain the technical principles of photon-counting CT in nonmathematical terms for radiologists and clinicians. Following a general overview of the current status of photon-counting CT, they will explain potential clinical applications of this technology.

© RSNA, 2018

- Dose reduction values of **32%, 34%, 36%, 60%** for various scenarios, also including patients.

Radiation Dose

During the past decade, the number of CT examinations increased yearly, with a 6.5% increase in the United States, resulting in a total of approximately 80 million CT scans per year (56,57). Despite the introduction of several dose-reducing techniques, such as iterative reconstruction, automatic exposure control, and electrocardiography-triggered imaging, radiation exposure remains a concern (58–60).

Image noise levels with photon-counting CT will be lower at the same level of x-ray exposure compared with conventional CT scanners because PCDs minimize electronic noise and enable optimal x-ray photon energy weighting (Fig 14). This can be used to reduce radiation doses. Kappler and colleagues (61) evaluated contrast and image noise by using water phantoms. They found increased iodine contrast with similar image noise compared with EID, resulting in a radiation dose reduction of up to 32%. Recent *in vivo* human experiments confirmed a dose reduction of up to 34% in photon-counting CT scans of the chest and brain (21,26).

Giersch et al (41) assessed the possibilities of energy weighting by simulating an ideal system. They found that images could be acquired with the same image quality using fewer photons, resulting in a radiation dose reduction by a factor of 2.5 (60% reduction). Photon-counting CT has the potential to improve CNR, which could be clinically used to reduce either the amount of contrast agent or the radiation dose (4,6,22). Compared with conventional CT, the smaller detector element size in photon-counting CT can be used for two different types of improvement, either increasing spatial resolution at a similar radiation dose and noise level or lowering radiation dose at a similar spatial resolution and noise level. This is because decreasing the detector element size means acquiring more data points. Even though this gives more noise in each individual detector element, the net result is that more high-spatial resolution information is obtained, which the reconstruction algorithm can translate to lower noise in the final images (38). A recent *in vivo* human study has shown that additional dose reduction of up to 36% is achievable with high-spatial-resolution photon-counting CT (39). Thus, it is likely that photon-counting CT will reduce radiation levels by approximately 30%–60%, depending on the imaging task.

Kappler et al.

First results from a hybrid prototype CT scanner for exploring benefits of quantum-counting in clinical CT

S. Kappler^a, T. Hannemann^a, E. Kraft^a, B. Kreisler^a,
D. Niederloehner^a, K. Stierstorfer^a, and T. Flohr^a

^a Siemens AG, Healthcare Sector, Siemensstr. 1, D-91301 Forchheim, Germany

ABSTRACT

We introduce a novel hybrid prototype scanner built to explore benefits of the quantum-counting technique in the context of clinical CT. The scanner is equipped with two measurement systems. One is a CdTe-based counting detector with 22cm field-of-view. Its revised ASIC architecture allows configuration of the counter thresholds of the 225 μ m small sub-pixels in chess patterns, enabling data acquisition in four energy bins or studying high-flux scenarios with pile-up trigger. The other one is a conventional GOS-based energy-integrating detector from a clinical CT scanner. The integration of both detection technologies in one CT scanner provides two major advantages. It allows direct comparison of image quality and contrast reproduction as well as instantaneous quantification of the relative dose usage and material separation performance achievable with counting techniques. In addition, data from the conventional detector can be used as complementary information during reconstruction of the images from the counting device. In this paper we present CT images acquired with the hybrid prototype scanner, illustrate its underlying conceptual methods, and provide first experimental results quantifying clinical benefits of quantum-counting CT.

- Dose reduction of up to **32%** due to the higher iodine contrast PC detectors provide.

To demonstrate the functionality of the hybrid prototype scanner and its underlying conceptual methods, we have recorded axial CT images of an anatomical phantom. To quantify the clinical benefits of counting detectors with small pixels, we have investigated contrasts, noise and dual-energy capability in 20cm water phantoms. At low counter thresholds, we could verify that Iodine contrast is increased by up to 20% (at 140kVp) while image noise is basically unaffected, all relative to the energy-integrating system. Merging the data from counters at 25keV and 55keV can further improve the Iodine CNR². **This allows to reduce patient dose by up to 32%** (at 140kVp). Dual-energy capability was demonstrated in a first quick study, confirming predictions from earlier CT image simulations. Continulative studies of the material separation properties of the quantum-counting detector including studies with up to four energy bins are planned in the near future.

Pourmorteza et al.

Photon-Counting CT of the Brain: In Vivo Human Results and Image-Quality Assessment

©A. Pourmorteza, ©R. Symons, ©D.S. Reich, ©M. Bagheri, ©T.E. Cork, ©S. Kappler, ©S. Ulzheimer, and ©D.A. Bluemke



ABSTRACT

BACKGROUND AND PURPOSE: Photon-counting detectors offer the potential for improved image quality for brain CT but have not yet been evaluated in vivo. The purpose of this study was to compare photon-counting detector CT with conventional energy-integrating detector CT for human brains.

MATERIALS AND METHODS: Radiation dose–matched energy-integrating detector and photon-counting detector head CT scans were acquired with standardized protocols (tube voltage/current, 120 kV(peak)/370 mAs) in both an anthropomorphic head phantom and 21 human asymptomatic volunteers (mean age, 58.9 ± 8.5 years). Photon-counting detector thresholds were 22 and 52 keV (low-energy bin, 22–52 keV; high-energy bin, 52–120 keV). Image noise, gray matter, and white matter signal-to-noise ratios and GM–WM contrast and contrast-to-noise ratios were measured. Image quality was scored by 2 neuroradiologists blinded to the CT detector type. Reproducibility was assessed with the intraclass correlation coefficient. Energy-integrating detector and photon-counting detector CT images were compared using a paired t test and the Wilcoxon signed rank test.

RESULTS: Photon-counting detector CT images received higher reader scores for GM–WM differentiation with lower image noise (all $P < .001$). Intrareader and interreader reproducibility was excellent (intraclass correlation analysis showed 12.8%–20.6% less image noise for photon-counting detector CT for GM and WM. The was 15.7% higher for GM–WM contrast and 33.3% higher for GM–WM contrast–

CONCLUSIONS: Photon-counting detector brain CT scans demonstrated greater contrast. This was due to both higher soft-tissue contrast and lower image noise

DISCUSSION

Photon-counting CT is a new development in CT scanning in which fully digital detectors replace crystals that emit light and photodetectors. In this study, objective measures of image quality showed that improvement ratios of PCD CT compared with EID were 12.8%–20.6% for image noise, 19.0%–20.0% for SNR, 15.7% for GM–WM contrast, and 33.3% for GM–WM CNR. These improvements in image quality were detected by experienced neuroradiologists blinded to the type of CT scan (conventional versus photon-counting CT). Neuroradiologists identified better GM–WM differentiation and less image noise on PCD images. These initial, in vivo human results for a prototype photon-counting CT suggest a high potential for PCD CT to improve image quality for brain CT compared with conventional detector CT. Alternatively, the lower image noise of the PCD CT system could translate to reduced radiation dose (approximately 40%) at similar quality levels of current brain CT.²⁴ Our results show that better GM–WM differentiation (CNR) with PCD versus EID CT is due to both higher GM–WM contrast and lower image noise. The improved contrast can be attributed to the better weighting of low-energy photons, which produce more contrast among soft tissues. The lower image noise in PCD was more visible in the mid-to-high frequencies of the noise-power spectrum.

- Brain imaging: dose reduction of approx. **40%** possible (iterative reconstruction).

Pourmorteza et al.

ORIGINAL ARTICLE

Dose Efficiency of Quarter-Millimeter Photon-Counting Computed Tomography First-in-Human Results

Amir Pourmorteza, PhD,*† Rolf Symons, MD,†‡ André Henning, PhD,§
Stefan Ulzheimer, PhD,§ and David A. Bluemke, MD, PhD||

Purpose: The aim of this study was to assess the clinical feasibility, image quality, and radiation dose implications of 0.25-mm imaging mode in a cohort of humans, achieved by dividing the photon-counting detector (PCD) size in half compared with standard-resolution photon-counting computed tomography (CT) (0.5 mm).

Methods: In this technical feasibility study, a whole-body prototype PCD-CT scanner was studied in the 0.25 mm detector mode (measured at isocenter). A high-resolution PCD-CT protocol was first tested in phantom and canine studies in terms of image noise and spatial resolution. Then, 8 human subjects (mean age, 58 ± 8 years; 2 men) underwent axial PCD 0.25-mm scans of the brain, the thorax, and at the level of the upper left kidney. Filtered backprojection reconstruction was performed with a sharp kernel (B70) for standard-resolution and high-resolution data at 0.5-mm isotropic image voxel. High-resolution data, in addition, were reconstructed with an ultrasharp kernel (U70) at 0.25-mm isotropic voxels.

Results: Image reconstructions from the PCD 0.25-mm detector system led to an improvement in resolution from 9 to 18 line pairs/cm in a line pair phantom. Modulation transfer function improved from 9.5 to 15.8 line pairs/cm at 10% modulation transfer function. When fully exploiting this improvement, image noise increased by 75% compared with dose-matched 0.5-mm slice PCD standard-resolution acquisition. However, when comparing with standard-resolution data at same in-plane resolution and slice thickness, the PCD 0.25-mm detector mode showed 19% less image noise in phantom, animal, and human scans.

Conclusion: High-resolution photon-counting CT in humans showed improved image quality in terms of spatial resolution and image noise compared with standard-resolution photon-counting.

Current clinical computed tomography (CT) scanners use energy-integrating detectors (EIDs) in which scintillator crystals absorb an incident x-ray photon and transform it to a number of light photons. Light sensors then convert the photons to electric current. Energy-integrating detector pixels are separated by optically isolating septa to avoid optical cross-talk. Although the EID crystals can be made smaller, the septa have a finite thickness that reduces the geometric efficiency of the detector. Therefore, there is a tradeoff between the size of EID pixels and their dose efficiency. The dimension of EID pixels has been limited to 0.9 to 1.0 mm, although recently, a 0.5-mm EID technology has been introduced.¹ Photon-counting detectors (PCDs) used in CT directly convert incident x-ray photons into charge clouds, which are then collected by an electronic array of anodes. With no scintillator and no septa, PCD pixels can be made smaller without compromising dose efficiency. Furthermore, reducing the pixel size of EIDs decreases the intensity of x-rays per pixel, which makes the detected electric current more susceptible to electronic noise. In contrast, although electronic and swank noise² affect the energy measurements in PCDs, they are effectively eliminated in counting of the photons.^{3,4} This might come at some cost in detection efficiency of very-low-energy photons, which are highly unlikely to have passed through the body.

It should be noted that simply increasing resolution (SR) CT projections into smaller images increase the spatial resolution of the system; the image voxel size (native voxel size) below which 1 of the system remains unchanged. Many factors affect the resolution, including x-ray focal spot size, reconstruction

and temporal bone in a healthy volunteer. The inner ear bones and the trabecular structures of the temporal bone are better visualized in the PCD-HR_{0.25} mode. Figure 6 shows examples of PCD-HR imaging of a region of normal lung and fibrotic lung. The results showed improved visualization of distal vessels and airways in PCD-HR_{0.25}. The PCD-HR_{0.5} images showed reduced image noise compared with SR acquisition. Additional examples of temporal bone and lung images of all volunteers are provided in the online appendix (Supplementary Fig. E2, Supplemental Digital Content 2, <http://links.lww.com/RLI/A380>, and Supplementary Fig. E3, Supplemental Digital Content 3, <http://links.lww.com/RLI/A381>).

DISCUSSION

We investigated the implications of 0.25-mm resolution mode of a photon-counting human prototype CT system in terms of image noise (or radiation dose) and spatial resolution. As expected, decreasing the detector pixel size by half compared with conventional CT resolution (0.5 mm) improved the spatial resolution as shown in phantom, animal,

- Radiation dose reduction up to **34%** (due to small pixels effect), B70f kernel

For many areas of the body, 0.5-mm resolution acquisitions may be adequate. However, PCD HR mode (0.25 mm) shows an intriguing advantage in this circumstance: acquiring at 0.25 mm with subsequent “downgrade” in reconstruction resolution to 0.5 mm resulted in approximately 19% lower image noise using PCD detectors. Image noise is proportional to the inverse square root of radiation dose at a fixed tube voltage.¹⁵ Alternatively, **radiation dose could be reduced by 34%** ($=1 - (1 - 0.19)^2$) for the PCD HR acquisition mode while still matching the noise characteristics of the SR (0.5 mm) mode. This phenomenon has been previously reported in detail by Baek et al¹⁶ and Tward and Siewersden¹⁷ for flat-panel detectors; in short, HR acquisition provides a better sampling of high-frequency CT noise and therefore reduces noise aliasing, that is, fold-over of high-frequency noise, which contaminates mid- and low-frequency features of the image. Therefore, we suggest the PCD-HR mode to be the default acquisition mode on the PCD scanner. The images may be reconstructed at greater than 0.5 mm isotropic voxel sizes for routine clinical assessment with lower noise compared with PCD-SR; in addition, they may be reconstructed at 0.25 mm isotropic voxel size to resolve smaller anatomical features.

Zhou et al.

ORIGINAL RESEARCH
HEAD & NECK

Comparison of a Photon-Counting-Detector CT with an Energy-Integrating-Detector CT for Temporal Bone Imaging: A Cadaveric Study

W. Zhou, J.I. Lane, M.L. Carlson, M.R. Bruesewitz, R.J. Witte, K.K. Koeller, L.J. Eckel, R.E. Carter, C.H. McCollough, and S. Leng

ABSTRACT

BACKGROUND AND PURPOSE: Evaluating abnormalities of the temporal bone requires high-spatial-resolution CT imaging. Our aim was to assess the performance of photon-counting-detector ultra-high-resolution acquisitions for temporal bone imaging and compare the results with those of energy-integrating-detector ultra-high-resolution acquisitions.

MATERIALS AND METHODS: Phantom studies were conducted to quantify spatial resolution of the ultra-high-resolution mode on a prototype photon-counting-detector CT scanner and an energy-integrating-detector CT scanner that uses a comb filter. Ten cadaveric temporal bones were scanned on both systems with the radiation dose matched to that of the clinical examinations. Images were reconstructed using a sharp kernel, 0.6-mm (minimum) thickness for energy-integrating-thicknesses for photon-counting-detector CT. Image noise was measured and compared blindly by 3 neuroradiologists to assess the incudomalleolar joint, stapes footplate, results for each specimen and protocol were compared using the Friedman test. The Krip-

RESULTS: Photon-counting-detector CT showed an increase of in-plane resolution on the same thickness (0.6 mm). Images from photon-counting-detector CT had significant energy-integrating-detector CT. Readers preferred the photon-counting-detector CT for all 3 temporal bone structures. A moderate interreader agreement was observed with quality, photon-counting-detector CT image sets were ranked significantly higher than ($P < .001$).

CONCLUSIONS: This study demonstrated substantially better delineation of fine anatomical structures on photon-counting-detector CT compared with the ultra-

with the EID-CT system. In this present work, with multiple cadaveric temporal bone specimens, we stated that with a clinical temporal bone reconstruction (U70), the PCD-CT UHR mode could achieve a 64% dose reduction compared with an EID-CT system when scanned at the same dose level and reconstructing at the same in-plane resolution (0.6 mm). The more aggressive noise reduction with the PCD-CT UHR mode compared with the previous report²³ is mainly due to the kernel difference (U70 is sharper than S80). Our study demonstrates the potential of a 64% reduction in dose using PCD-CT for clinical temporal bone imaging to achieve the same image quality as EID-CT. This finding confirmed the previous conclusion that

MATERIALS AND METHODS

Phantom Experiments to Evaluate Spatial Resolution

A 50- μm diameter tungsten wire inserted into a solid water phantom was scanned along the z-axis on the whole-body PCD-CT scanner using the UHR scan mode. The PCD-CT system was built on the platform of a second-generation dual-source CT scanner (Somatom Definition Flash; Siemens). Detailed descriptions of this system have been reported elsewhere.¹²⁻¹⁴ The UHR acquisition on the PCD-CT system has an effective pixel size of 0.25×0.25 mm at the isocenter.²³ PCD-CT scans were obtained with the following parameters: spiral mode, 120-kV tube potential, 25- and 75-keV energy thresholds, 32×0.25 mm collimation, 0.8 pitch, and 1.0-second rotation time. For comparison, the wire phantom was also scanned on a second-generation dual-source CT scanner, the same platform on which the PCD-CT was built. Both the PCD-CT and EID-CT systems involved in this study use an identical UHR focal spot size of 0.7 mm.²⁸ **EID-CT scans were obtained using the standard clinical protocol: UHR mode with a comb filter along the fan direction.** spiral mode, 120-kV tube potential, 16×0.6 mm collimation, 0.8 pitch, and 1.0-second rotation time. All images were reconstructed with a standard weighted filtered back-projection algorithm, 0.6-mm slice thickness, and a sharp kernel (U70). Modulation transfer function (MTF) is commonly used to provide a comprehensive evaluation of spatial resolution for imaging systems by assessing the system response with respect to the input signal at each frequency. In this study, the MTF was calculated from the point spread function of

- Dose reduction of **64%** for temporal bone imaging (U70f kernel).
- Comparison between PC-UHR and EI detector with a comb filter.

Rajendran et al.

ORIGINAL ARTICLE

Dose Reduction for Sinus and Temporal Bone Imaging Using Photon-Counting Detector CT With an Additional Tin Filter

Kishore Rajendran, PhD,* Benjamin A. Voss, MD,* Wei Zhou, PhD,* Shengzhen Tao, PhD,* David R. DeLone, MD,* John I. Lane, MD,* Jayse M. Weaver, BA,* Matthew L. Carlson, MD,† Joel G. Fletcher, MD,* Cynthia H. McCollough, PhD,* and Shuai Leng, PhD*

the PCD-CT acquisition. The average noise reduction across all the inserts was 26.2%, whereas the image contrast between PCD-CT (Sn-100 kV) and EID-CT (120 kV) were comparable (Fig. 2C). Using Eq. 1, the dose reduction from Sn-100 kV PCD-CT was calculated to be 56.5% if matched image noise is targeted. The results from the multienergy phantom experiment demonstrate that Sn-100 kV PCD-CT could be used as an alternative to 120-kV EID-CT with the potential to reduce dose if matched image noise and contrast is targeted for a given reconstruction kernel.

Energy-integrating detector CT and PCD-CT images from the

mean dose reduction of 67%. The 10- and 8-mGy sinus patient images from clinical EID-CT for visualization of critical 2 and $P = 0.01$ for lesser palatine foramina, 39 for nasomaxillary sutures, and median anterior ethmoid artery canal). The 6- and show any significant difference between 0 (sharp kernel, 10% modulation transfer from a sinus patient scan increased the compared with the clinical EID-CT images. The rated a dose reduction of up to 85% compared visualization of inner ear structures similar between EID-CT and PCD-CT. studies demonstrated dose reduction using current clinical EID-CT while maintaining resolution was further validated in sinus and temporal bone visualization capability from PCD-CT on for sinus imaging compared with cur-

- Comparison between PC-UHR+Sn 100 kV (CountT) and EI 120 kV (Flash)
- A UHR mode with comb filter was used (only) for the temporal bone cadaver scan on the EID-CT.
- Phantom: Dose reduction of up to 56.5% (H70 kernel)

Cadaver:

- Sinus protocol : dose reduction of 67% (H70)
- Temporal bone protocol (EI with comb filter): dose reduction of 83% (U70)

TABLE 2. CT Acquisition and Reconstruction Parameters Used in the Phantom and Cadaver Experiments

Acquisition System	Multienergy CT Phantom		Anthropomorphic Head Phantom		Cadaver Head	
	EID-CT*	PCD-CT†	EID-CT*	PCD-CT†	EID-CT*	PCD-CT†
Protocol	Sinus	Sinus UHR	Sinus	Sinus UHR	T-bone UHR‡	T-bone UHR
Tube potential, kV	120	100	120	100	120	100
Additional tin filter	No	Yes, 0.4 mm	No	Yes, 0.4 mm	No	Yes, 0.4 mm
Energy thresholds, keV	—	25, 65	—	25, 65	—	25, 65
Tube-current-time product, mAs	88	545	71	500	215	500
Pitch	0.55	0.55	0.60	0.60	0.60	0.60
CTDI _{vol} (16 cm)	13.5	10.8	13.5	10.1	48§	10.1
Collimation, mm	64 × 0.6	32 × 0.25	64 × 0.6	32 × 0.25	8 × 0.6	32 × 0.25
Rotation time, s	1	1	1	1	1	1
Reconstruction kernel	H70	H70	H70	H70	U70	U70
Slice thickness, mm	0.75	0.75	0.75	0.75	0.6	0.6
Reconstruction FOV, mm	275	275	275	275	80	80
Image matrix size	512 × 512	512 × 512	1024 × 1024	1024 × 1024	512 × 512	512 × 512

*Definition Flash.

†Somatom Count.

‡EID-based UHR is enabled using comb filter.

§CTDI_{vol} estimated using CareDose4D (Siemens Healthcare).

CT indicates computed tomography; PCD-CT, photon-counting detector computed tomography; EID-CT, energy-integrating detector computed tomography; UHR, ultra-high-resolution; FOV, field of view.

Klein et al.

ORIGINAL ARTICLE

Effects of Detector Sampling on Noise Reduction in Clinical Photon-Counting Whole-Body Computed Tomography

Laura Klein, BS,*† Sabrina Dorn, MS,*‡ Carlo Amato, MS,*† Sarah Heinze, MD,§ Monika Uhrig, MD,* Heinz-Peter Schlemmer, MD,* Marc Kachelrieß, PhD,*‡ and Stefan Sawall, PhD*‡

Objectives: Reconstructing images from measurements with small pixels below the system's resolution limit theoretically results in image noise reduction compared with measurements with larger pixels. We evaluate and quantify this effect using data acquired with the small pixels of a photon-counting (PC) computed tomography scanner that can be operated in different detector pixel binning modes and with a conventional energy-integrating (EI) detector.

Materials and Methods: An anthropomorphic abdominal phantom that can be extended to 3 sizes by adding fat extension rings, equipped with iodine inserts as well as human cadavers, was measured at tube voltages ranging from 80 to 140 kV. The images were acquired with the EI detector (0.6 mm pixel size at isocenter) and the PC detector operating in Macro mode (0.5 mm pixel size at iso) and ultrahigh-resolution (UHR) mode (0.25 mm pixel size at iso). Both detectors are components of the same dual-source prototype computed tomography system. During reconstruction, the modulation transfer functions were matched to the one of the EI detector. The dose-normalized contrast-to-noise ratio (CNRD) values are evaluated as a figure of merit.

Results: Images acquired in UHR mode achieve on average approximately 6% higher CNRD compared with Macro mode at the same spatial resolution for a quantitative D40f kernel. Using a sharper B70f kernel, the improvement increases to 21% on average. In addition, the better performance of PC detectors compared with EI detectors with regard to iodine imaging has been evaluated by comparing CNRD values for Macro and EI. Combining both of these effects, a CNRD improvement of up to 34%, corresponding to a potential dose reduction of up to 43%, can be achieved for D40f.

Conclusions: Reconstruction of UHR data with a modulation transfer function below the system's resolution limit reduces image noise for all patient sizes and tube voltages compared with standard acquisitions. Thus, a relevant dose reduction may be clinically possible while maintaining image quality.

Key Words: tomography, x-ray computed tomography, contrast media, iodine, phantoms, imaging, radiation dosage, photon-counting CT

Invest Radiol 2020;55: 111-119

converts the incoming x-ray photons directly into a measurable charge cloud with the resulting signal amplitude being proportional to the energy of the incident photon.⁵ This direct conversion results in a signal with a very small full width at half maximum (FWHM) in the order of tens of nanoseconds.^{6,7} In combination with the usage of rather small pixels, it is possible to distinguish single photons and register their energies accordingly. These small-sized pixels and the small FWHM are necessary to account for the high x-ray flux rates of clinical computed tomography (CT) systems. Otherwise, pulse pile-up, that is, the detection of multiple photon counts as a single event, would be too predominant and limit the performance of the detectors in clinical practice.⁴ In contrast, conventional energy-integrating (EI) detectors use a scintillation material (typically Gd₂O₂S) to convert the x-ray photons to optical photons, which are then measured by photo-diodes.⁸ The amplitude of the resulting current is also energy dependent, but the FWHM of the signal is about a factor 100 higher than for PC detectors. Therefore, the measured photo-current is integrated over the measurement time in case of EI detectors. Also, the usage of even smaller pixels than the typical slice collimations found in CT (eg, 0.5 mm, 0.6 mm, or 0.625 mm, depending on model and vendor) is difficult to realize due to the necessity of reflecting lamellae required in EI detectors between the detector pixels to minimize cross-talk and to guide the optical photons to the photodiodes, but seems to have been realized lately by one manufacturer in a detector with 0.25 mm slice collimation.⁹ However, because these required reflecting lamellae cannot be manufactured arbitrarily small, this leads to a decreasing active area of the detector, that is, a decreasing geometric efficiency, with decreasing pixel size, resulting in decreasing dose efficiency. This is no problem for PC detectors as the sensor layer is made of one continuous crystal. Compared with EI detectors, PC detectors promise to provide significant improvements and possible new applications, that is, multienergy acquisition with 2 or more energy bins within a single scan, improved material decomposition, and the possibility to discriminate multiple contrast agents simul-

- Dose reduction due to small pixels: **31%** for B70f.
- Dose reduction due to small pixels + iodine: up to **43%** for D40f and up to **63%** for B70f.

DISCUSSION

In this study, systematic measurements of phantoms and human cadavers have been performed to quantify the effect of noise reduction by acquisitions with small detector pixels and reconstruction to a lower spatial resolution compared with acquisitions with larger pixels, resulting in the same MTF. Although the resulting MTFs were shown to match for the investigated protocols, reconstructions from data acquired with small pixels resulted in noticeably lower image noise potentially allowing for a corresponding dose reduction. A comparison of the results in phantoms between Macro and UHR allows for estimating the dose reduction in the order of about 10% on average for the D40f kernel. The improvement on noise is even higher using a sharper kernel, resulting in a potential dose reduction of about 31% on average for B70f. The results presented herein are consistent with the ones achieved for measurements using 120 kV in earlier publications and using sharp convolution kernels.^{15,24} As these benefits are theoretically expected to hold even for EI detectors, this might also be of particular interest considering recently announced clinical scanners with smaller pixels.²⁵

acquisition with smaller detector pixels. Combining both of these major benefits, PC detectors provide CNRD improvements of up to 34.3% and 66.7%, respectively, resulting in a potential dose reduction of up to 43.3% and 63.4%, respectively, for the kernels D40f and B70f investigated herein.

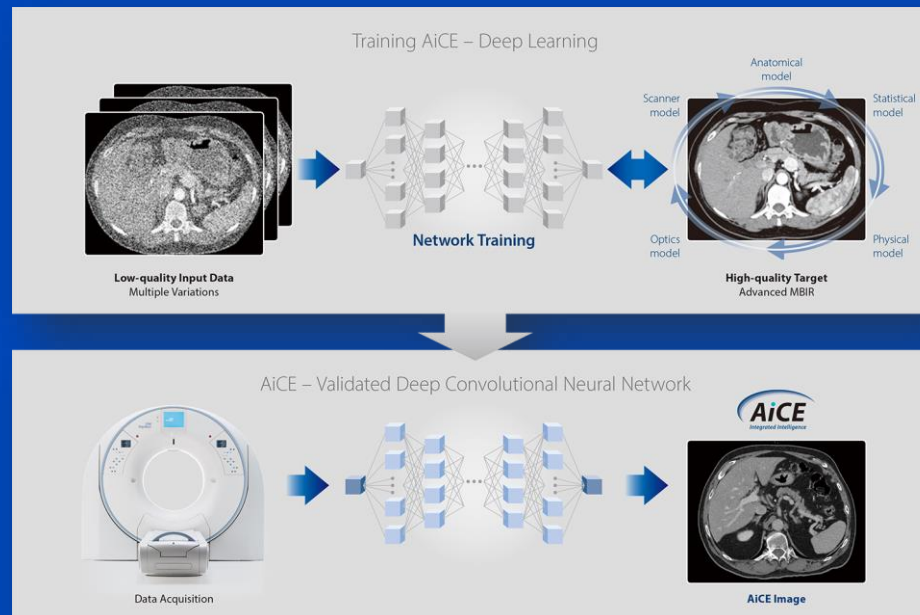
Dose Reduction by Photon Counting

- Reasons for less dose
 - Better iodine contrast
 - Energy bin weighting
 - UHR without comb
 - Smaller pixels
 - ...

In general, it seems realistic that a **dose reduction of 30% or more** can be achieved in clinical routine.

Dose Reduction by Deep Learning

- Not many clinical studies exist
 - Canon's AiCE shown 20% noise reduction (36% less dose) compared to AIDR 3D in coronary CTA¹
 - Canon's AiCE outperforms AIDR 3D which outperforms FIRST in lesion detection². It further outperforms FIRST which outperforms AIDR 3D noise-wise²: Average dose reduction (taken from noise reduction) compared to FIRST is 38%.



Information taken from https://global.medical.canon/products/computed-tomography/aice_dlr

¹Tatsugami et al. Deep learning-based image restoration algorithm for coronary CT angiography. *EuRad* 29:5322-5329, 2019

²Singh et al., Image Quality and Lesion Detection on Deep Learning Reconstruction and Iterative Reconstruction of Submillisievert Chest and Abdominal CT. *AJR* 214:566-573, March 2020

Dose Reduction by Deep Learning

Region	Noise DL	Noise Iterative	Dose Reduction DL to Iterative	Ref.
Liver	11.4 HU	16.2 HU	51%	[1]
Subcutaneous fat	9.9 HU	13.2 HU	44%	[1]
Paraspinal muscle	9.9 HU	14.5 HU	54%	[1]
Abdominal aorta	11.11 HU	15.5 HU	48%	[1]
Abdomen	SNR = 5.08	SNR = 2.93	69%	[2]
Phantom			9% to 17% DLR-L, 46 to 56% DLR-H compared to AV50 (IR with 50% dose level)	[3]
Coronary Artery	42%	100% (ASiR70)	66% compared to ASiR70	[4]
Abdomen			61% compared to MBIR 67% compared to HybridIR	[5]
Full body			50% compared to FBP	[6]

10% or significantly more dose reduction can be seen.

- [1] Shin YJ, Chang W, Ye JC, et al. Low-Dose CT with Deep Learning: Comparison with CT Reconstructed with Filtered Back Projection or Iterative Reconstruction. *Investigative Radiology*. 2019;54(10):754–761.
- [2] A. Heinrich, M. Engler, N. D. D. et al. Deep Learning for Low-Dose CT: A Comparison with CT Reconstructed with Filtered Back Projection or Iterative Reconstruction. *Proceedings of the 2019 IEEE International Symposium on Biomedical Imaging (ISBI)*. 2019;1–5.
- [3] Greffier et al. Image quality and dose reduction in low-dose CT: A phantom study. *EurRad* 30(7), 2020
- [4] R. R. Buechel, D. C. Benz, G. et al. Deep learning improves image quality of abdominal ultra-high-resolution CT. *Eur Radiol* 29, 6163–6171 (2019).
- [5] Akagi, M., et al. Deep learning improves image quality of abdominal ultra-high-resolution CT. *Eur Radiol* 29, 6163–6171 (2019).
- [6] Andrew D. Missert, et al. Noise Subtraction for Low-Dose CT Images Using a Deep Convolutional Neural Network. *Proceedings of the CT-Meeting 2018*.

Total Dose Reduction

Additionally Possible Compared to Today's CTs

- Risk-specific AEC (Joscha Maier)
 - about **10%**, depending on the tube voltage
- Optimized spectra (Michael McNitt-Gray and)
 - **20%** to 50% depending on object size
- Dynamic bowtie (Grace Gang)
 - **27%** to 50%
- Photon counting (literature):
 - **30%**
- Deep learning replacing iterative recon
 - **10%** to 30%
- **The additional future dose reduction potential is conservatively estimated to be round about 70%.**
 - $1 - (1 - 10\%) \cdot (1 - 20\%) \cdot (1 - 27\%) \cdot (1 - 30\%) \cdot (1 - 10\%) = 67\%$

	Child (15 cm × 10 cm)	Adult (30 cm × 20 cm)	Obese (50 cm × 40 cm)
Soft tissue, Sn	0.5 mm / 20× / 15%	1.0 mm / 20× / 32%	2.7 mm / 20× / 51%
Soft tissue, Cu	1.2 mm / 20× / 16%	3.9 mm / 20× / 32%	7.5 mm / 20× / 50%
Iodine, Sn	0 mm / 1× / 0%	0.2 mm / 13× / 14%	0.6 mm / 20× / 31%
Iodine, Cu	0.4 mm / 20× / 32%	0.8 mm / 20× / 34%	1.0 mm / 20× / 41%

Steidel, Kachelrieß et al., RSNA 2020

Outlook

- **Vendors:**
 - Implement those measures and bring them into clinical routine
- **Medical physicists and radiologists:**
 - Use the new technology to reduce patient dose
 - Or use it to improve image quality

Thank You!



The 6th International Conference on Image Formation in X-Ray Computed Tomography

August 3 - August 7 • 2020 • Regensburg (virtual only) • Germany • www.ct-meeting.org



© Bild Regensburg Tourismus GmbH

Conference Chair: **Marc Kachelrieß**, German Cancer Research Center (DKFZ), Heidelberg, Germany

This presentation is available at www.dkfz.de/ct.

Job opportunities through DKFZ's international Fellowship programs (marc.kachelriess@dkfz.de)
Parts of the reconstruction software were provided by RayConStruct® GmbH, Nürnberg, Germany.

